

Dual-metamaterial silicon micro-ring resonators

(Student Paper)

T. T. D. Dinh¹, X. Le Roux¹, J. Zhang¹, M. Montesinos¹, C. Lafforgue^{1,2}, D. Benedikovic¹, P. Cheben^{3,4}, E. Cassan¹, D. Marris-Morini¹, L. Vivien¹, and C. Alonso-Ramos¹

¹ Université Paris-Saclay, Univ. Paris-Sud, CNRS, Centre de Nanosciences et de Nanotechnologies, 91120, Palaiseau, France

² École Normale Supérieure Paris-Saclay, Université Paris-Saclay, 94230 Cachan, France

³ National Research Council Canada, ON K1A0R6 Ottawa, Canada

⁴ Center for Research in Photonics, University of Ottawa, Ottawa K1N6N5, Canada

e-mail: Dinh.Thi-Thuy-Duong@c2n.upsaclay.fr

ABSTRACT

Subwavelength metamaterial engineering has opened exciting prospects for controlling and manipulating light in silicon photonic waveguides. Most state-of-the-art subwavelength photonic waveguides rely on periodic nanostructuring of the core or the cladding, but not both. Here, we present a new waveguide geometry that exploits metamaterial engineering of the core and the cladding, independently. By implementing two metamaterials, this step-index geometry provides unique flexibility in the design of the waveguide index contrast. The proposed approach opens additional degrees of freedom to shape single-mode condition and to control modal confinement in the vertical and horizontal directions. Hence, the proposed dual-metamaterial waveguide geometry has a great potential for applications requiring optimized light-matter interactions such as sensing, hybrid integration or nonlinear wavelength conversion. As a proof-of-concept, we experimentally demonstrate dual-metamaterial micro-ring resonators in the 220-nm-thick Si technology with quality factors in excess of 50000 near 1550 nm wavelength.

Keywords: silicon photonics, subwavelength, light-matter interactions, sensing.

1. INTRODUCTION

Periodically patterning silicon with a pitch small enough to suppress diffraction effects has proven to be a simple and powerful tool to control the propagation of light in photonic waveguides [1-3]. Since the first demonstration of Si waveguide with subwavelength grating core [1], a great number of SWG-assisted devices have been proposed and demonstrated to achieve state-of-the-art performance [2,3]. Subwavelength grating (swg) waveguides are promising to shape modal light confinement, which could be instrumental for applications requiring tight control of light matter interactions like sensing, hybrid integration of active materials or nonlinear wavelength conversion. Most state-of-the-art swg waveguides rely on metamaterial engineering of the core [4-8] or the cladding [9,10], but not both. In these geometries, the index of the cladding or the core is fixed, thereby limiting the flexibility in controlling the modal confinement. In waveguides with a subwavelength metamaterial cladding only, the evanescent field is limited by the tight confinement in the central silicon strip. On the other hand, in waveguides with a subwavelength metamaterial core, the maximum waveguide width is set by single-mode operation. Then, the minimum effective metamaterial that can be implemented is restricted by leakage to the substrate, limiting the maximum evanescent field [11]. Subwavelength waveguides interleaving shifted silicon strips have been recently proposed that implement different metamaterials in the core and the cladding. However, the same silicon strips define the core and cladding geometry, limiting the flexibility in the design of the index contrast. Here, we propose and experimentally demonstrate a new waveguide geometry that implements different subwavelength metamaterials in the core and the cladding. This strategy enables flexible control of the synthesized metamaterial indices in the core and the cladding, independently, thereby relaxing the requirements for single-mode condition. Then, comparatively wider waveguides still afford single-mode operation, which alleviates restrictions in minimum effective metamaterial index. As a first demonstration of the potential of this approach, we have fabricated silicon micro-ring resonators implemented with single-mode dual-metamaterial waveguides with thickness of 220 nm and core width as large as 900 nm. The ring resonators exhibit measured quality factors in excess of 50000 and extinction ratio larger than 15 dB near 1550 nm wavelength. These results compare favorably with previously reported silicon resonators based on subwavelength nano-structuration, that showed quality factors on the order of 10000 [7,13].

2. WAVEGUIDE DESIGN

The geometry of the proposed dual-metamaterial waveguide is schematically shown in Fig. 1(a). The holes in the core and cladding have the same longitudinal and transversal periods of $\Lambda_L = 200$ nm and $\Lambda_T = 450$ nm,

respectively. The holes in the waveguide core have a length of $L_{\text{core}} = 100$ nm and a width of $W_{\text{core}} = 100$ nm, while the holes in the cladding have a length of $L_{\text{cladding}} = 100$ nm and a width of $W_{\text{cladding}} = 250$ nm. The silicon layer thickness is 220 nm. In each longitudinal period the waveguide comprises two holes in the core and 14 holes at each side of the cladding. We have considered silica as under- and upper-cladding materials.

The transverse-electric (TE) polarized modes typically have a strong field near the vertical waveguide walls, where the sidewall roughness is. This may result in high propagation loss. To avoid this issue, we choose to work with the transverse-magnetic (TM) polarized mode. We have calculated the electric field distribution of the fundamental TM mode near 1550 nm wavelength using three-dimensional finite difference time domain (3D-FDTD) simulations. The electric field distribution at the planes α and β (described in Fig. 1(a)) are shown in Figs. 1(b) and (c), respectively. The TM mode has an effective index of ~ 1.9 , and carries more than 70% of the electric field intensity outside the silicon.

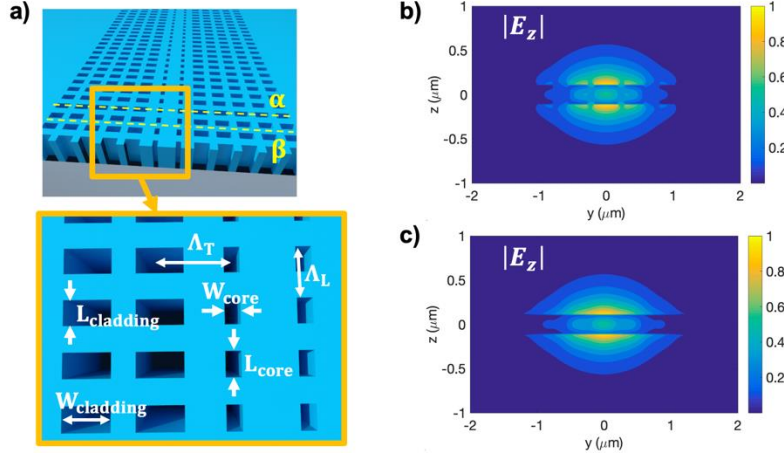


Figure 1. a) Schematic view of the proposed dual-metamaterial waveguide. Electric field distributions of the fundamental TM mode near 1550 nm wavelength for a waveguide with $L_{\text{core}}=100$ nm, $W_{\text{core}}=100$ nm, $L_{\text{cladding}}=100$ nm and $W_{\text{cladding}} = 200$ nm, along b) the plane α and c) the plane β , as marked in panel a).

To study the single mode condition in the proposed waveguide we used the two-dimensional metamaterial waveguide model, as illustrated in Fig. 2(a). The metamaterials in the core and cladding are substituted by their equivalent effective index ($n_A = 3.36$, $n_B = 3.19$). We calculated the effective index for the fundamental and first order TM modes at 1550 nm wavelength as a function of the waveguide width, W . As shown in Fig. 2(b), the waveguide is single mode for a waveguide width below 1 μm . For comparison, the single-mode limit for conventional strip waveguide is near 500 nm. For a waveguide with subwavelength metamaterial core the single mode limit is near 600 nm.

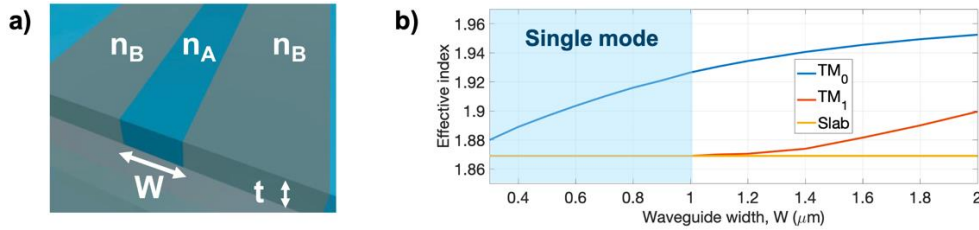


Figure 2. a) Schematic two-dimensional model of the dual-metamaterial waveguide. The subwavelength metamaterial structures in the core and cladding are modelled by their equivalent refractive indices, n_A and n_B . b) Effective index of the fundamental (TM_0) and first order (TM_1) order TM modes, calculated as a function of the waveguide width, W . The blue region indicates width satisfying the single-mode condition.

3. EXPERIMENTAL DEMONSTRATION

To demonstrate the feasibility of the proposed approach, we have fabricated and experimentally characterized several ring resonators, implemented in the 220-nm-thick silicon platform with buried oxide (BOX) layer of 3 μm . The patterns were defined using electron-beam lithography and dry etching. Fabricated rings are cladded with PMMA to symmetrize the structure. The bus waveguide and the ring resonator are implemented with the dual-metamaterial waveguide with $L_{\text{core}} = 100$ nm, $W_{\text{core}} = 100$ nm, $L_{\text{cladding}} = 100$ nm and $W_{\text{cladding}} = 200$ nm. The micro-rings have a radius of 80 μm .

Figure 2(a) shows a scanning electron microscope image of one of the fabricated rings. The transmittance spectra for a ring resonator with a gap of 800 nm is shown in Fig. 2(b). From the lower envelope of the resonances, it can be concluded that the critical coupling is achieved near 1580 nm wavelength. In the critical coupling region,

the extinction ratio is ~ 25 dB and the quality factor (Q) is ~ 23000 , as shown in Fig. 3(c). At shorter wavelengths, the ring is in the under-coupling regime, with a higher Q of ~ 55000 dB and an extinction ratio exceeding 15 dB.

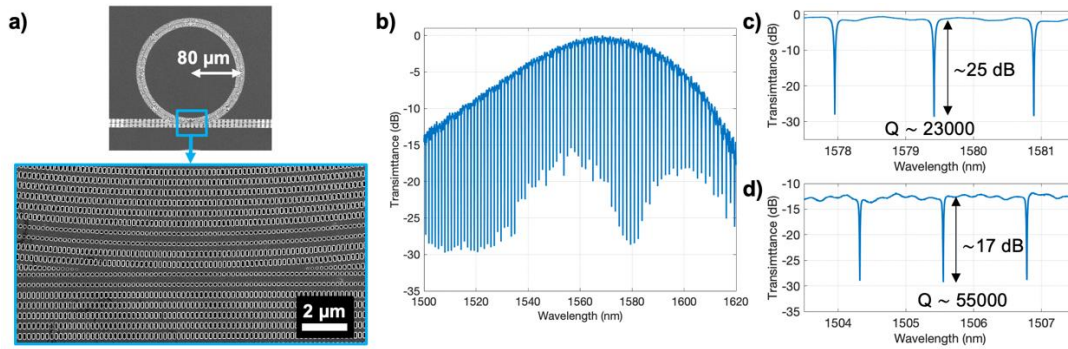


Figure 3. a) Scanning electron microscope image of fabricated ring. b) Transmittance spectrum of the ring resonator for TM polarization. Detail of the ring transmittance in c) critical coupling and d) under-coupling regimes.

4. CONCLUSIONS

We have proposed and experimentally demonstrated a new kind of waveguide geometry that implements two different metamaterials in the core and the cladding. This dual-metamaterial geometry provides new degrees of freedom to engineer the single-mode condition and the vertical and lateral field confinements. By judiciously designing the synthesized metamaterial indices in the core and cladding, we ensure single-mode operation for a waveguide width as large as $1 \mu\text{m}$. Our 3D-FDTD simulations showed that for the fundamental TM mode of a waveguide with a width of 900 nm (within the single-mode regime), more than 70% of the electric field intensity propagates outside the silicon. To experimentally validate the feasibility of the proposed approach, we have fabricated dual-metamaterial ring resonators, exhibiting high quality factors exceeding 50000, among the highest values reported for silicon subwavelength ring resonators [7,13]. We believe that these results open a new route for the implementation of advanced modal confinement engineering in silicon photonic devices.

ACKNOWLEDGEMENTS

Agence Nationale de la Recherche (MIRSPEC ANR-17-CE09-0041, BRIGHT ANR-18-CE24-0023-01).

REFERENCES

- [1] P.J. Bock, *et al.*: Subwavelength grating periodic structures in silicon-on-insulator: a new type of microphotonic waveguide, *Opt. Express*, vol. 18, pp. 20251-20262, 2010.
- [2] R. Halir, *et al.*: Waveguide sub-wavelength structures: a review of principles and applications, *Laser Photonics Rev.*, vol. 8, pp. 25-49, 2015.
- [3] P. Cheben, *et al.*: Subwavelength integrated photonics, *Nature*, vol. 560, pp. 565-572, 2018.
- [4] J.G. Wangüemert-Pérez, *et al.*: Evanescent field waveguide sensing with subwavelength grating structures in silicon-on-insulator, *Opt. Lett.*, vol. 39, pp. 4442-4445, 2014.
- [5] V. Donzella, *et al.*: Design and fabrication of SOI micro-ring resonators based on sub-wavelength grating waveguides, *Opt. Express*, vol. 23, pp. 4791-4803, 2015.
- [6] H. Yan, *et al.*: Unique surface sensing property and enhanced sensitivity in microring resonator biosensors based on subwavelength grating waveguides, *Opt. Express*, vol. 24, pp. 29724-29733, 2016.
- [7] D. Benedikovic, *et al.*: Sub-wavelength silicon grating metamaterial ring resonators, in *Proc. GFP 2017*, Berlin, Germany, Aug. 2017.
- [8] E. Luan, *et al.*: Enhanced sensitivity of subwavelength multibox waveguide microring resonator label-free biosensors, *IEEE J. Sel. Top. Quantum Electron.*, vol. 25, pp. 7300211-1-7300211-11, 2018.
- [9] J. Soler Penadés, *et al.*: Suspended SOI waveguide with sub-wavelength grating cladding for mid-infrared, *Opt. Lett.*, vol. 39, pp. 5661-5664, 2014.
- [10] W. Zhou, *et al.*: Fully suspended slot waveguides for high refractive index sensitivity, *Opt. Lett.*, vol. 42, pp. 1245-1248, 2017.
- [11] J.D. Sarmiento-Merenguel, *et al.*: Controlling leakage losses in subwavelength grating silicon metamaterial waveguides, *Opt. Lett.*, vol. 41, pp. 3443-3446, 2016.
- [12] B. Taurel, *et al.*: Sub-wavelength grating interdigitated combs as photonic waveguides, *Opt. Lett.*, vol. 44, pp. 3869-3872, 2019.
- [13] J.G. Wangüemert-Pérez, *et al.*: Subwavelength structures for silicon photonics biosensing, *Opt. Laser Technol.*, vol. 109, pp. 437-448, 2019.